

# The feasibility of a generalized passive shimming construct for human brain imaging

Dennis F R Heijtel<sup>1,2</sup>, Jacco A de Zwart<sup>2</sup>, Peter van Gelderen<sup>2</sup> and Jeff H Duyn<sup>2</sup>

<sup>1</sup>Biomedical NMR, Department of Biomedical Engineering, Eindhoven University of Technology, the Netherlands

<sup>2</sup>Advanced MRI, LFMI, NINDS, National Institutes of Health, Bethesda, MD, USA

## Introduction

Static magnetic field inhomogeneities negatively affect image quality, increasingly so at high magnetic field strength. In human brain imaging, active shim coils cannot adequately compensate for these spatial field perturbations due to the limited number of degrees of freedom available. Passive shimming has been previously demonstrated on a per subject basis<sup>1,2,3</sup>, however it is not practically feasible in day-to-day scanning of volunteers or patients.

Since both the placement of the head in tight fitting coil arrays and the head shape are fairly constant over experiments, we investigated the feasibility of generalized passive shimming based on a cylindrical array of ferrous particles, placed between the transmit coil and receive coil array. Two questions are addressed: How reproducible is the field over different volunteers (after 2<sup>nd</sup> order active shim), and can an array of solely paramagnetic particles consistently improve homogeneity?

## Materials & Methods

All measurement were conducted on a GE (Milwaukee, WI) Signa 7 T whole body MRI with a 32-channel receive-only detector array (Nova Medical, Wilmington, MA) and Nova transmit coil. Initially, EPI-based field maps used for higher-order shimming were used to determine the residual field inhomogeneities over volunteers (see abstract<sup>4</sup>), however signal loss in certain areas (e.g. frontal brain) was too severe. Therefore, post-shimming field maps (Gradient Echo: FOV= 240x180x126 mm<sup>3</sup>; matrix=128x96x32; TR=1 s; TE=6.5/9.2 ms) were used instead. The mean field map over the volunteers (n=15) and standard error of this mean (used as weighting factor after smoothing over 5 voxels) were computed.

Given the large diameter of the defined grid, solely paramagnetic elements can be used in practice (steel shim stock, Lyon industries, South Eglin, IL). Constrained least squares fitting was used to determine the iron distribution on a cylindrical grid of 512 evenly spaced elements (16 rings of 32 elements,  $\varnothing=28$  cm,  $z=24$  cm, see Fig. 1), with additional regressors for  $B_0$ , 1st and 2nd order shim terms (9 regressors). To investigate the theoretically achievable performance the fit was repeated allowing for diamagnetic materials as well. Residual field histograms were computed, with the frequency range as quantification for the  $B_0$  homogeneity and the standard deviation over the volunteers as indicator of the scan to scan variability.

## Results

Fig. 2 shows the average field map over volunteers and the standard error of this mean. Only voxels that were inside the brain in 4 or more volunteers were taken into account. The result of the fit (Fig. 3d, 17 non-zero particles) was used to correct the field in the mean map (Fig. 3a) as well as the field in the original data on a volunteer-by-volunteer basis (Fig. 3b-c). Histograms of the residual field distribution are shown in Fig. 3a-b: For uncorrected data (black), with the proposed paramagnetic-only correction (red) and using a bipolar correction (para- and diamagnetic particles) (green). The bipolar fit performs better when fitting the mean over volunteers (the frequency range containing 80% of the voxels was reduced to 0.54 and 0.74 times the width of uncorrected data for the bipolar and paramagnetic fit respectively, Fig. 3a). However, this difference is insignificant when using fit results to compensate the field in individual data (relative 80%-width of  $0.83 \pm 0.6$  for dipolar,  $0.73 \pm 0.6$  for diamagnetic, Fig. 3b).



Figure 1: Pictures of the proposed passive shimming construct currently being constructed. The shim elements will be mounted on an acrylic cylinder inserted between the transmit and receive-array coils (left). A 16x32 grid of particles is used (right).

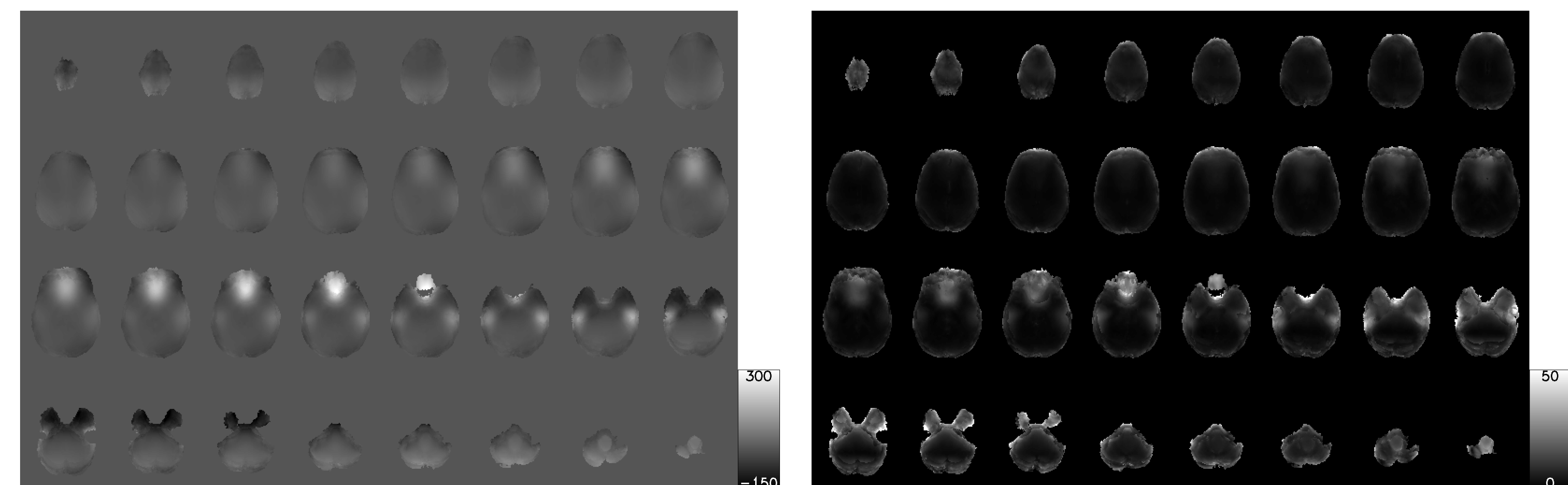


Figure 2: The average field map over 15 different volunteers (left), and the standard error of this mean (right), both in Hz.

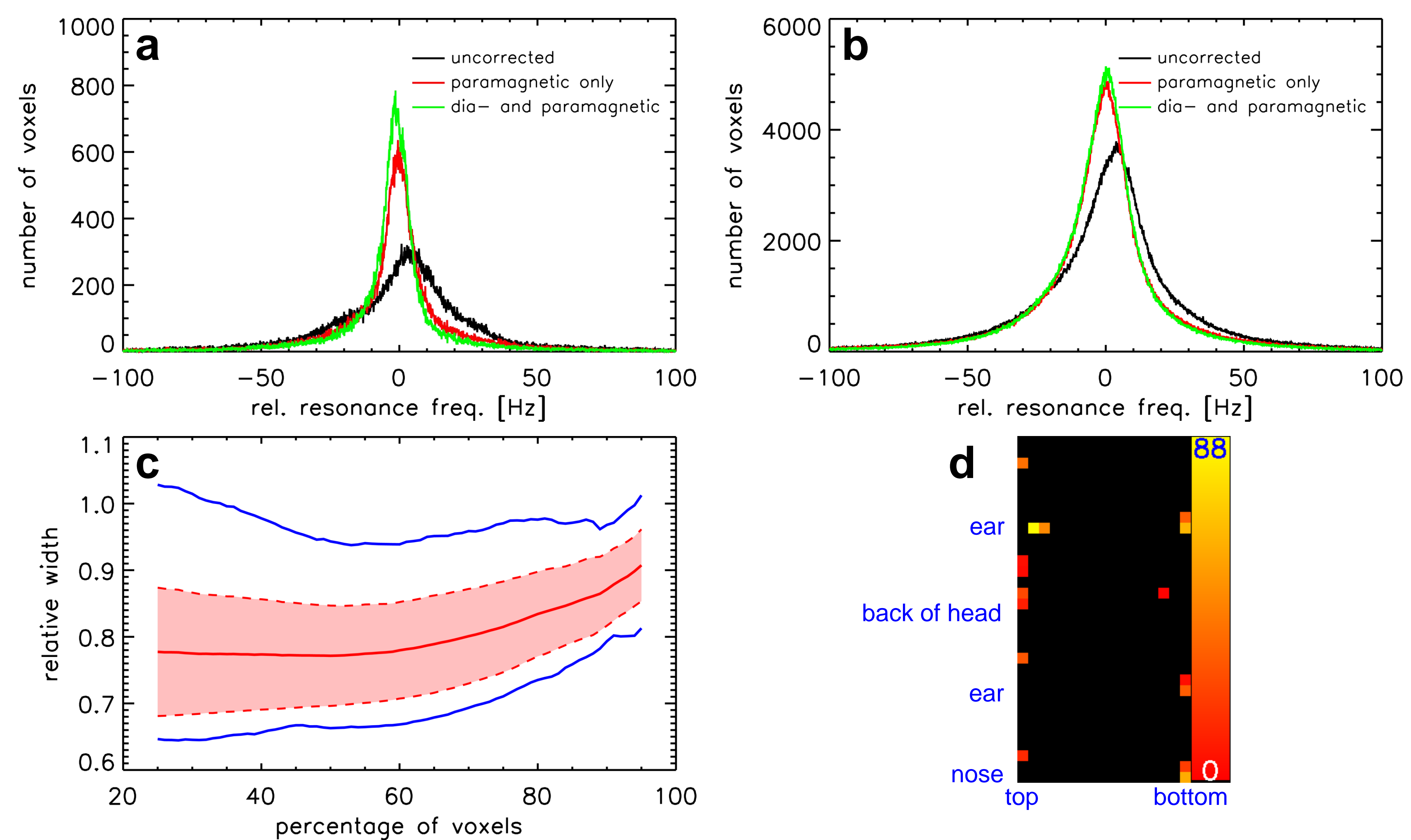


Figure 3: Field distribution histograms for corrected and uncorrected data for the mean over volunteers (a) and all of the individual datasets (b). The relative width of the paramagnetic-only histogram compared to the uncorrected histogram is shown in red in (c). Standard deviation (dashed) and the extremes (blue) are also shown. The fitted particle distribution in mg of iron is shown in (d).

Fig. 3c shows the relative width of the residual field after paramagnetic correction compared to uncorrected data for the central (least amount off-resonance) 25% to 95% of all voxels. The mean and standard deviation over 15 volunteers are shown in red, whereas the best (lowest relative width) and worst (highest relative width) performing volunteer are shown in blue, demonstrating that the shimming construct increases field homogeneity in virtually all cases.

## Conclusion

Based on preliminary data, the use of a generalized passive shimming approach is feasible, with an overall average improvement in field homogeneity of approximately 17%. Field-homogeneity improvements are found for all volunteers, however volunteer-to-volunteer variability was found to be the biggest source of variance. Experimental validation and evaluation of benefits for practical imaging applications are currently underway.

## References

- [1] K.M. Koch et al., Proc. 15<sup>th</sup> ISMRM, Berlin, Germany, 2007, p 982
- [2] J.L. Wilson et al., Neuroimage 19 (2003) 1802-1811
- [3] A. Jesmanowicz et al. US Patent 6,294,972 B1 (2001)
- [4] D.F.R. Heijtel et al., Proc 17<sup>th</sup> ISMRM, Honolulu, HI, USA, 2009, p 3077